# Signal Theoretical Aspects of Bistatic SAR

Joachim H. G. Ender
FGAN-FHR, Neuenahrer Str. 20, D-53343 Wachtberg, Germany
Tel: +49 228 9435-323, Fax: +49 228 9435-618, E-Mail: ender@fgan.de

*Abstract*— **Bistatic SAR uses separated transmitter and receiver flying on different platforms. This configuration is envisaged to achieve benefits like the exploitation of additional information contained in the bistatic reflectivity of targets, reduced vulnerability in military systems or forward looking SAR imaging. The feasibility of the bistatic concept was already demonstrated by experimental investigations.**

**Nevertheless, a closed satisfying theory reaching from signal modelling over the data collection strategies and the analysis of possible imaging performance to the specification of processors for practical use does not yet exist. The reason may be found in the non-standard geometry resulting in radar signals of high complexity.**

**In this paper, we will start from a signal model for a rather general configuration. Since the changing imaging geometry makes it difficult to derive a general processor, we first look over the well known classes of monostatic SAR-processors. Then, the inversion problem is formulated for the bistatic case resulting in the matched filter processor. Emanating from this, two techniques are derived which are locally optimum either for short apertures or for small scenes. Special attention is turned to the transfer of range-migration type algorithms to the bistatic case.**

## I. Introduction

There is not much open literature treating bistatic SAR processing. Some special aspects are already addressed in the paper [2]. In [1] bistatic spotlight SAR is regarded from a tomographic point of view. [6] describes the special case of a two-dimensional geometry and parallel flight paths allowing to apply an approximative application of the range-migration algorithm. [7] and [8] treat a time domain technique as well as a k-domain approach for the special case of a fixed transmitter. Lastly, [4] introduces a fast backprojection technique in a two-dimensional geometry. To the author's knowledge, a general modelling in three dimensions including an evaluation of representative processing approaches has not yet been published.

## II. Geometry and General Signal Model

### A. General geometry

We look at the geometrical situation as sketched in Fig. 1. The instantaneous position of the transmit antenna phase centre T is denoted by $\mathbf{R}_t(\xi)$, that of the receive antenna R by $\mathbf{R}_r(\xi)$ (of course, the roles of transmit and receive antennas can be exchanged without effect to the radar signals). $\xi$ parametrises the paths of the two antennas: for instance, it can be the slow-time itself or the spatial covered distance of one of the antennas or of their common centre of gravity.

We assume a spotlight situation; t. i., the beams of both antennas are directed towards a scene fixed beam focus point

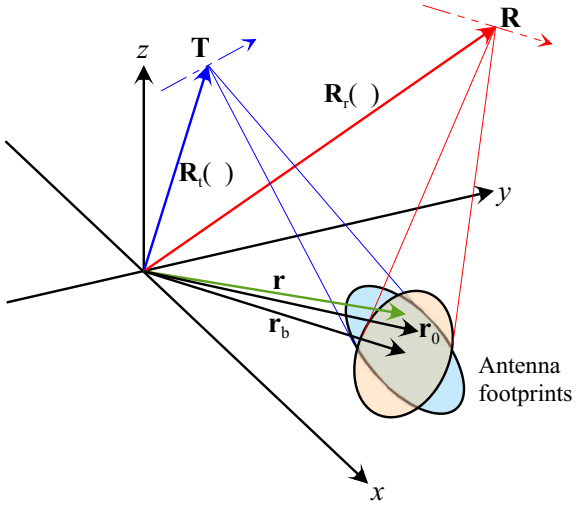


Fig. 1. Bistatic Geometry

$\mathbf{r}_b$. Another scene fixed point $\mathbf{r}_0$ serves as a reference point.[1] Further, we regard an arbitrary point scatterer at the position $\mathbf{r} = (x, y, z)^t$ within the intersection $I$ of the transmit and receive antenna footprint. The $(x, y)$-plane is considered to be the local approximation of the earth's surface.

We define the *bistatic range history* of this scattering point at $\mathbf{r}$ by

$$R(\xi; \mathbf{r}) = |\mathbf{R}_t(\xi) - \mathbf{r}| + |\mathbf{R}_r(\xi) - \mathbf{r}|. \tag{1}$$

In the bistatic situation, the range history can be quite unusual, even for straight motions of transmitter and receiver (see Fig. 2), so hyperbolic or parabolic approximations have to be applied only with great care!

### B. Equi-range and Equi-rangeslope

The sets of all points with a fixed range $r$, or a fixed rangeslope $v$, respectively, are denoted by

$$M_r(\xi, r) = \{\mathbf{r} : R(\xi; \mathbf{r}) = r\} \tag{2}$$

$$M_v(\xi, v) = \left\{\mathbf{r} : \frac{\partial}{\partial \xi} R(\xi; \mathbf{r}) = v\right\} \tag{3}$$

and their cuts with the $(x, y)$-plane by $\mathcal{M}_r(\xi, r)$ and $\mathcal{M}_v(\xi, v)$. As generally known, $M_r(\xi, r)$ turns out to be an ellipsoid with the two focal points at the places of transmitter

[1] To generalise the derivation to stripmap like configurations, $\mathbf{r}_b$ and $\mathbf{r}_0$ could be also functions of $\xi$; nevertheless, we will concentrate on the spotlight situation.

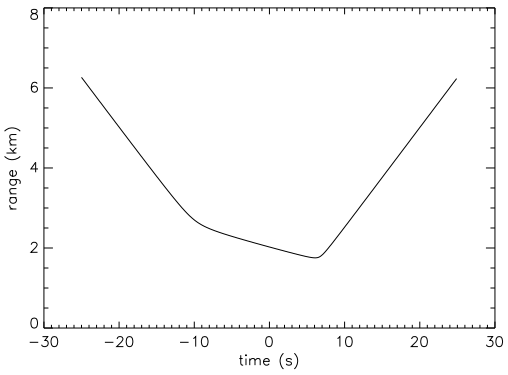


Fig. 2. Example of a bistatic range history for constant velocities

and receiver, so $\mathcal{M}_r(\xi, r)$ will be ellipses as cuts of an ellipsoid with a plane (*"Equi-range lines"*).

The derivative of the bistatic range with respect to the path parameter $\xi$ can be expressed by:

$$\frac{\partial}{\partial \xi} R(\xi; \mathbf{r}) = \frac{\partial}{\partial \xi} \left( |\mathbf{R}_t(\xi) - \mathbf{r}| + |\mathbf{R}_r(\xi) - \mathbf{r}| \right) \quad (4)$$

$$= \mathbf{u}_t^t(\xi) \frac{\partial}{\partial \xi} \mathbf{R}_t(\xi) + \mathbf{u}_r^t(\xi) \frac{\partial}{\partial \xi} \mathbf{R}_r(\xi) \quad (5)$$

In this expression, the unit vectors

$$\mathbf{u}_t(\xi) = \frac{\mathbf{R}_t(\xi) - \mathbf{r}}{|\mathbf{R}_t(\xi) - \mathbf{r}|} \quad \mathbf{u}_r(\xi) = \frac{\mathbf{R}_r(\xi) - \mathbf{r}}{|\mathbf{R}_r(\xi) - \mathbf{r}|} \quad (6)$$

point to the line of sights of the transmitter resp. receiver to the scatterer. The set $M_v(\xi, v)$ is given by the union of all intersections of such "velocity cone"-pairs, whose sum of receiver and transmitter range slopes are equal to $v$. The cut $\mathcal{M}_v(\xi, v)$ with the $(x, y)$-plane determines the *"equi-rangeslope lines"*.

The momentary imaging grid on the plane is formed by these equi-range and equi-rangeslope lines. It may be rather complicated exhibiting in many cases the possibility to image also in the direction of motion for one or both of the two radar platforms (see Fig. 3).

### C. Signal model

The spectrum of the transmitted signal $s_t(t)$ within one pulse covers a certain frequency band $[f_1, ...f_2]$ corresponding to a band of wave-numbers $[k_{r,1}, ..., k_{r,2}]$ with $k_r = 2\pi f/c$, and $c =$ velocity of light. The received signal from a single scatterer is - if the platform motion during one pulse is neglected - in good approximation a time-delayed version of $s_t$. If the measured signal is Fourier transformed to the range frequency domain, inversely filtered over the frequency band $[f_1, ...f_2]$, (t.i. divided by the Fourier transform of the transmitted signal), and if a variable substitution is performed replacing the range frequency by the range wave-number, we get the normalised signal from this scatterer:

$$s(\xi, k_r; \mathbf{r}) = e^{-jk_r R(\xi; \mathbf{r})}. \quad (7)$$

The antenna pattern has been neglected in this expression, which can be justified by the spotlight assumption. The same model can be applied, if the data are taken directly in the frequency domain e.g. by a stepped frequency wave form or by de-ramping.

We now look at a reflectivity distribution denoted by $a(\mathbf{r})$. This will be concentrated normally to the $(x, y)$-plane but could also be carried by a vaulted area or even be distributed three-dimensional. The signal of all scatterers is the superposition of the individual contributions:

$$z(\xi, k_r) = \int_I s(\xi, k_r; \mathbf{r}) a(\mathbf{r}) d\mathbf{r}. \quad (8)$$

If we apply a Fourier transformation along $\xi$, we get

$$Z(k_\xi, k_r) = \iint_I e^{-jk_r R(\xi; \mathbf{r}) - jk_\xi \xi} a(\mathbf{r}) d\mathbf{r} d\xi \quad (9)$$

$$= \int_I K\left(k_\xi, k_r, \mathbf{r}\right) a(\mathbf{r}) d\mathbf{r} \quad (10)$$

$$\text{with } K\left(k_\xi, k_r, \mathbf{r}\right) = \int e^{-jk_r R(\xi; \mathbf{r}) - jk_\xi \xi} d\xi. \quad (11)$$

We will call $k_\xi$ the *path-wavenumber*, thinking of $\xi$ as a covered distance. The integral kernel $K$ defines an operator $\mathcal{O}$ from the space of all admitted reflectivity distributions into the space of signals in the $(k_\xi, k_r)$-domain.

## III. The Inversion Problem

The SAR processor can be regarded as an operator in the opposite mapping direction coming close to the inversion of $\mathcal{O}$. In the following, we will discuss several approaches generalising well-known monostatic processors.

### A. Classes of monostatic processors

The *matched filter processor* (MFP) optimises the signal-to-noise-ratio and offers an optimum but computational inefficient solution. For each pixel of the image, the signal expected from a scatterer at this place is complex conjugated, multiplied to the measured data and summed up. The *local aperture optimum processor* (LAP) approximates the MFP for short apertures yielding an image of in principle non limited size with a coarse azimuth resolution. It is close to the *range-Doppler processor* which starts with a range-compression and then works along the range bins separately. The *local image optimum processor* (LIP) approximates the MFP in a small region around an image point. It results in a polar reformatting scheme in the monostatic case. The *backprojection processor* (BP) performes a successive image formation after range-compression by projecting the range lines from the appropriate direction onto the image plane. The computational effort of this technique can be decreased by *fast backprojection processing* (FBP) techniques. One of the most popular technique is the *range-migration processor* (RMP) combining near-optimum performance with high numerical efficiency (see [3]). The key step of the RMP is formed by an interpolation in the k-space.

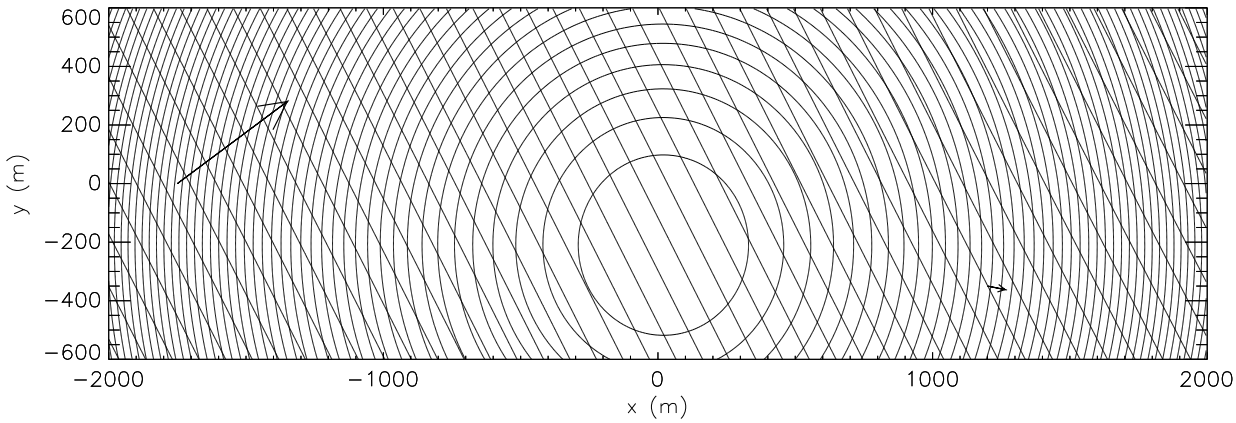


Fig. 3. Example for a momentary bistatic image grid. The arrows symbolise the position and velocity of transmitter and receiver. The transmitter (left) moves at an altitude of 15 km with a 7.5 times larger velocity than the receiver at an altitude of 10 km; no vertical velocity components

### *B. The bistatic matched filter processor*

We now want to extend these classes of monostatic processors to the bistatic case. The MFP can be used to study the achievable imaging performance determined by the bistatic geometry. Starting from Eq. (8) the maximum SNR is achieved by the inversion formula

$$\hat{a}(\mathbf{r}) = C \iint z(\xi, k_r) e^{jk_r R(\xi;\mathbf{r})} d\xi dk_r, \tag{12}$$

provided that the superposed noise is white over $\xi$ and $k_r$. Apart from the more complicated range history, there is no difference to the monostatic case. The MFP also can be applied in the $k_r - k_x$ domain:

$$\hat{a}(\mathbf{r}) = C \iint Z(k_\xi, k_r) K^*(k_\xi, k_r, \mathbf{r}) dk_\xi dk_r. \tag{13}$$

### *C. The bistatic local image optimum processor*

The bistatic LIP is based on the approximation of the expected signal in a small region $B$ around a reference point $\mathbf{r}_0$. The maximum extension of $B$ is given by the condition, that receiver and transmitter are in the far field of $B$. If this is fulfilled, the signal in Eq. 7 can be approximated by

$$s(\xi, k_r; \mathbf{r}) \approx e^{-jk_r R(\xi;\mathbf{r}_0)} e^{-jk_r \frac{\partial}{\partial \mathbf{r}} R(\xi;\mathbf{r})|_{\mathbf{r}=\mathbf{r}_0}(\mathbf{r}-\mathbf{r}_0)}. \tag{14}$$

With

$$\frac{\partial}{\partial \mathbf{r}} R(\xi; \mathbf{r}) = (\mathbf{u}_t(\xi) + \mathbf{u}_r(\xi))^t \tag{15}$$

the image formation results in

$$\hat{a}(\mathbf{r}) = C \int\int e^{j2k_r \mathbf{u}_{eff}^t (\mathbf{r}-\mathbf{r}_0)} z(\xi, k_r) d\xi dk_r \tag{16}$$

with the *effective LOS vector* $\mathbf{u}_{eff}(\xi) = \frac{1}{2}(\mathbf{u}_t(\xi) + \mathbf{u}_r(\xi))$.

Introducing the new variable $\mathbf{k} = 2k_r \mathbf{u}_{eff}$ and reformatting the measured values to a function $\tilde{z}(\mathbf{k})$ according to $\tilde{z}(2k_r \mathbf{u}_{eff}(\xi)) = z(\xi, k_r)$, this equation simplifies to a common Fourier transform

$$\hat{a}(\mathbf{r}) = C \int_{\mathcal{K}} e^{j\mathbf{k}(\mathbf{r}-\mathbf{r}_0)} \tilde{z}(\mathbf{k}) \mathbf{dk}. \tag{17}$$

The set $\mathcal{K}$ ("k-set", see [5]), over which the integration is performed, is composed of all vectors $2k_r \mathbf{u}_{eff}(\xi)$, where $k_r$ runs through the wave-numbers of the emitted waveform and $\xi$ through an interval determining the part of the synthetic aperture used for the image formation. If the scene is assumed to be flat, it is sufficient to regard the two-dimensional projection of $\mathcal{K}$ to the $(x, y)$-plane.

The shape of $\mathcal{K}$ (or its projection) can be quite different from that known from the monostatic case. The local form of the point spread function at $\mathbf{r}_0$ is given by the (possibly windowed) back transform of the indicator function of the k-set. Since the bistatic LIP is locally identical to the MFP, this analysis can also serve as a tool to study the global imaging performance by variation of $\mathbf{r}_0$.

### *D. The bistatic local aperture optimum processor*

If only a small part of the aperture is used, a Taylor expansion of the range history around the variable $\xi_0$ at the centre of the used aperture part can be performed up to the first or second degree:

$$\begin{aligned} R(\xi, \mathbf{r}) \quad &\approx \quad R(\xi_0, \mathbf{r}) + R'(\xi_0, \mathbf{r})(\xi - \xi_0) \\ &\quad \left[ + \frac{1}{2} R''(\xi_0, \mathbf{r})(\xi - \xi_0)^2 \right]. \end{aligned} \tag{18}$$

The prime and double prime here stand for the first and second derivatives with respect to $\xi$. If the approximation is performed only to the first order, the MFP simplifies to a range-Doppler processor with linear range-walk compensation, while the treatment of the second order approximation for arbitrary geometries imposes similar problems as the general solution.

### *E. Bistatic backprojection processing*

According to Eq. 13, the integration along $k_r$ may be performed for each $\xi$ resulting in a range-compressed signal $Z(\xi, r)$. The second integral sums up all the contributions from the different points of the path:

$$\hat{a}(\mathbf{r}) = \int Z(\xi, R(\xi; \mathbf{r})) d\xi. \tag{19}$$

This integral can be carried out by adding from pulse to pulse the relating contributions from the range compressed signal for each pixel of the later image. Note, that the principle is the same as in the monostatic case, but the mapping $\mathbf{r} \rightarrow R(\xi;\mathbf{r})$ is more complicated.

### *F. Bistatic range-migration processing*

The simple and efficient scheme of the monostatic RMP cannot be transferred to the bistatic situation by a simple means. In our approach, we try to hold the assumptions as general as possible, intending to come to satisfying solutions at least for special geometrical situations. So, the focused image is not forced to a rectangular grid; we are content, if we get it well focused, a further step then is to ortho-rectify the image by interpolation. We introduce a second vector variable $\mathbf{q}$ which is related to the original scene coordinate variable $\mathbf{r}$ via an invertible mapping $\mathbf{T}$ with $\mathbf{T}(\mathbf{q}) = \mathbf{r}$. The reflectivity now is regarded as a function of the new variable $\mathbf{q}$. So, with $I' = \mathbf{T}^{-1}(I)$, Eq. 9 can be re-arranged to

$$\begin{aligned} Z(k_\xi, k_r) &= \iint_{I'} e^{-jk_r R(\xi;\mathbf{T}^{-1}(\mathbf{q}))-jk_\xi\xi} a(\mathbf{q}) d\mathbf{q} d\xi \\ &= \int_{I'} K(k_\xi, k_r, \mathbf{q})\, a(\mathbf{q}) d\mathbf{q} \end{aligned} \quad (20)$$

with the modified kernel

$$\begin{aligned} K(k_\xi, k_r, \mathbf{q}) &= \int e^{-jk_r R(\xi;\mathbf{T}^{-1}(\mathbf{q}))-jk_\xi\xi} d\xi \quad (21) \\ &= \int e^{-jk_r [R(\xi;\mathbf{T}^{-1}(\mathbf{q}))+\zeta\xi]} d\xi \quad (22) \end{aligned}$$

and $\zeta := k_\xi / k_r$. To simplify the kernel, we apply the principle of stationary phase. We define

$$F(\xi, \zeta, \mathbf{q}) := R(\xi, \mathbf{T}^{-1}(\mathbf{q})) + \zeta\xi \quad (23)$$

and assume that there exists an unique $\xi_0(\zeta, \mathbf{q})$ with

$$\frac{\partial}{\partial\xi} F(\xi, \zeta, \mathbf{q})|_{\xi=\xi_0(\zeta,\mathbf{q})} = 0. \quad (24)$$

For this $\xi_0(\zeta, \mathbf{q})$ we find the phase $-k_r G(\zeta, \mathbf{q})$ with $G(\zeta, \mathbf{q}) = F(\xi_0(\zeta, \mathbf{q}), \zeta, \mathbf{q})$ and the kernel can be simplified to

$$K(k_\xi, k_r, \mathbf{q}) \approx e^{-jk_r G(\zeta,\mathbf{q})}, \quad (25)$$

if the amplitude is neglected.

The properties of $G(\zeta, \mathbf{q})$ determine, wether the approximated kernel can be used to transfer the imaging equations to a Fourier based processor.

We define: The kernel is called *separable*, if there exist a vector valued function $\mathbf{w}(\zeta)$ and a scalar function $G_0(\zeta)$ with $G(\zeta, \mathbf{q}) = G_0(\zeta) + \mathbf{w}^t(\zeta)\mathbf{q}$. If the kernel is separable, Eq. 20 can be written as

$$\begin{aligned} Z(\zeta k_r, k_r) &\approx e^{-jk_r G_0(\zeta)} \int_{I'} exp\left\{-jk_r \mathbf{w}^t(\zeta)\mathbf{q}\right\} a(\mathbf{q}) d\mathbf{q} \\ &= e^{-jk_r G_0(\zeta)} A(k_r \mathbf{w}(\zeta)), \end{aligned} \quad (26)$$

where $A(.)$ is the Fourier transform of $a(.)$. Now, the data $Z(k_\xi, k_r)$ can be re-sampled to a rectangular grid for the new wave-number domain $\mathbf{k_q} = k_r \mathbf{w}(k_\xi / k_r)$ and back-transformed to the $\mathbf{q}$-domain after removing the phase introduced by $G_0$. The last step is to reverse the application of the mapping $\mathbf{T}$, t. i. to interpolate the image to the original $\mathbf{r}$-domain. The processing chain is sketched in Fig. 4

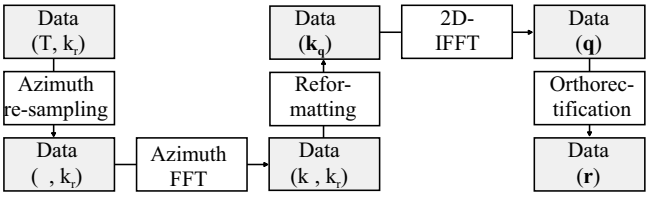


Fig. 4. Range migration processing

The main question is, for which geometrical situations it is possible to find a parametrisation $\xi$ of the flight paths and a mapping $\mathbf{T}$ producing a separable kernel (which is no problem for the monostatic case). Since it is difficult (or impossible) to find a closed formula for $G(\zeta, \mathbf{q})$, numerical representations have to be used. Numerical techniques also can serve for a good approximation by a separable kernel.

## IV. Conclusion

In this paper, a general description of the bistatic SAR-signals for a three-dimensional geometry was given. Several archetypes of processors were sketched pointing out the commonness and discrepancies to the monostatic case. Clearly, for practical applications the integral formulations have to be transferred to the discrete Fourier transformations with care. For the range migration processor - which is proposed often as the most appealing approach for the monostatic case - a rather general framework was outlined for the bistatic situation which still has to be filled with concrete applications.

## Acknowledgment

This work is funded by the German Federal Ministry of Defense (BMVg) and the Federal Office of Defense Technology and Procurement (BWB).

## References

[1] Arikan, O., Munson, D.C.: "A tomographic formulation of bistatic synthetic aperture radar", Intern. Conf. on Advances in Communicartion and Control Systems 1988, Baton Rouge, La., pp. 289 - 302

[2] Ausherman, D., et al.: "Developments in radar imaging", IEEE Trans. Aerosp. Electron. Syst., vol. 20, p. 363-400, July 1984

[3] Cararra, W.G. et al.: "Spotlight synthetic aperture radar", Artech House, 1995

[4] Ding, Y., Munson, D. C.: "A fast back-projection algorithm for bistatic SAR imaging", IEEE Intern. Conf. on Image Proc., Rochester, Sept 2002

[5] Ender, J.H.G.:"The meaning of k-space for classical and advanced SAR-techniques", PSIP'2001, Marseilles, January 2001

[6] Soumekh, M.: "Bistatic synthetic aperture radar inversion with application in dynamic object imaging", IEEE Trans. on Signal Processing, Vol. 39, No. 9, Sept. 1991, pp. 2044-2055

[7] Soumekh, M.: "Bistatic synthetic aperture radar imaging using wide-bandwidth continuous-wave sources", SPIE Conference on Radar Processing Technology and Applications, San Diego, California, July 1998, pp. 99-109

[8] Soumekh, M.: "Wide-bandwidth continuous-wave monostatic/bistatic synthetic aperture radar imaging", International Conference on Image Processing, Chicago, Oct. 1998, pp, 361-364